THE ASTROPHYSICAL JOURNAL, 303:119–129, 1986 April 1

A SIMPLE MODEL FOR COUPLED CONVECTION AND PULSATION

R. F. STELLINGWERF
Mission Research Corporation
Received 1985 April 18; accepted 1985 October 1

ABSTRACT

A generalization of Baker's one-zone pulsation model is derived that includes a simple treatment of time-dependent convection. Both nonlinear and linear effects are discussed. It is shown that even this "first-order" approach yields interesting results. The convective flux tends to stabilize the pulsation, most effectively for red models. The turbulent pressure is always destabilizing, with the most effective phasing for "instability strip" models (i.e., those with convective time scale equal to the dynamic time scale). It is also shown that this model is subject to a number of dynamic instabilities that could cause problems for generalized time-dependent mixing length formulations.

Subject headings: convection — hydrodynamics — stars: interiors — stars: pulsation

I. INTRODUCTION

The treatment of convection in pulsating stars has proven to be a major theoretical stumbling block in recent years. An understanding of this problem is badly needed to predict accurately the width of the instability strip, the modal transition lines, and the dependence of pulsation parameters on stellar parameters, most notably the helium abundance. Several attempts to apply a generalized mixing length theory to this problem have failed because of unexpected instabilities. In this paper a very simple model of the convection/pulsation interaction is studied with the aim of better understanding the pitfalls of this problem.

Convection has two effects on pulsating stars: (1) modification of the static structure of the star (reducing the temperature gradient in the outer layers), and (2) modification of the time dependence (phase) of the flux in the outer layers. Baker and Kippenhahn (1965) included convective effects of the first type in models of Cepheids and found that the structural changes in the stars caused a neutralization of the pulsational instability in very cool models, but this effect occurred far to the red of the observed red edge of the instability strip. It thus appears that the observed stabilization of stars at the red edge must be caused primarily by the time-dependent convective effects.

The early Cepheid models computed by Cox, Brownlee, and Eilers (1966) and Cox *et al.* (1966) included convection via a "phase lag" equation, in which the rate of change in the convective flux is limited to the eddy circulation time, and the limiting value is taken to be that of the mixing-length theory of Böhm-Vitense (1958). The effects of convection are not discussed in these papers, however, and the convective flux was eventually dropped from the calculation (King *et al.* 1973). Later work by Baker and Gough (1979) and Gonczi (1981, 1982) showed that such a scheme is subject to an instability that causes unphysical fluctuations in the convective flux as a function of radius. This means that, although the time dependence of the convection may be reasonable, the assumption that the convection is determined completely locally is not, and some type of average over a mixing length is needed to make the theory reasonable and stable.

The first computational models to demonstrate the quenching effect of convection at the red edge were the two-dimensional computations of Deupree (1977*a–d*). Later, Stellingwerf (1982*a*, *b*, 1984*a–c*) obtained similar results using a spherical model with nonlocal convection included via a diffusion term, and again using a phase-lag type of equation for the principal time dependence. These models also predict a convective effect near the blue edge, but it is a destabilizing effect for these hotter models. It seems that the effects of convection in pulsating stars can be of either sign, rather than a purely stabilizing influence.

It is clearly desirable to understand this process at a more fundamental level than detailed code results. The one-zone model developed by Baker (1966) contributed an understanding of pulsational instability mechanisms, and it is clear, since the structural effects of convection seem to be of less importance than the time dependence, the the one-zone approach should be helpful here as well. Another motivation is the possibility of studying more complicated types of behavior with the one-zone model, such as aperiodic oscillations (Baker, private communication) and hysteresis effects (Auvergne, Baglin, and Morel 1981). Such a model was described previously by Unno and Kamijo (1966) and Gough (1967), who found a possible destabilization for very cool (long-period) variables. General properties of the problem have been discussed recently by Pesnell (1985).

Poyet and Spiegel (1979) analyze the pulsation/convection problem in an approach that is complimentary to the present analysis: they consider the effects of pulsation as a perturbation to the problem of *convective* instability, with the possibility of an anharmonic driving motion. Here we derive the effects of convection as a perturbing influence on *pulsational* instability including the anharmonic effects arising from the nonlinear equation of motion.

In this paper, we derive the simplest form of a convective one-zone model: the original Baker model supplemented by a convective flux whose time variation is given by a phase-lag equation for the turbulent velocity. The resulting system is first derived in simple nonlinear form, and then linearized, in § II. In the following section a stability analysis of the system, which is fourth order in time, is described, and in § V nonlinear models are discussed.

II. DERIVATION OF THE MODEL

a) *Radiative Case*

The present one-zone treatment differs from Baker's original derivation in two respects: (1) the model is generalized to describe a shell of arbitrary thickness comprising the outer layer of a spherical star; (2) we derive the model first as a simplified set of nonlinear equations, and then do the linear (small-amplitude) analysis. The model has been derived in this form in Stellingwerf (1972; hereafter S72) whose notation will usually be followed here. In that paper it was shown that this thin-shell one-zone model is a very good representation of an instability strip variable star both in its stability properties and in its nonlinear behavior.

Consider a spherical homogeneous shell of outer radius r and inner radius r_c. Its inner surface is fixed, while its outer surface is free to move, but has an equilibrium position, r_0. Defining $X = r/r_0$, we write

$$\frac{\rho}{\rho_0} = X^{-m} , \tag{1}$$

$$\frac{P}{P_0} = \left(\frac{\rho}{\rho_0}\right)^{\Gamma_1} H = X^{-m\Gamma_1} H , \tag{2}$$

$$\frac{T}{T_0} = X^{-m(\Gamma_1 - 1)} H , \tag{3}$$

where

$$m = \frac{3}{1 - (r_c/r_0)^3} , \tag{4}$$

$$\Gamma_1 = \left(\frac{\partial \ln P}{\partial \ln \rho}\right)_s , \tag{5}$$

for the density, pressure, and temperature in the shell as functions of the surface displacement, assuming perfect gas. The function H embodies all nonadiabatic effects, and is determined by the energy equation. Reasonable values of $\Gamma_1 \approx 1.1$ and $m \approx 10$ for an unstable Cepheid model. We define

$$q = m\Gamma_1 - 2 \approx 9 , \tag{6}$$

and take as the unit of time the free-fall time:

$$\tau = t/t_{\rm ff} , \tag{7}$$

$$t_{\rm ff} = \left(\frac{GM}{r_0^3}\right)^{-1/2} . \tag{8}$$

Since the external values of quantities such as pressure and temperature are small, the spatial derivatives of these quantities are proportional to the quantity itself. This is equivalent to assuming that logarithmic derivatives of quantities are simple constants.

The radiative luminosity is thus

$$\frac{L_r}{L_0} = X^4 \left(\frac{T}{T_0}\right)^4 \left(\frac{\kappa}{\kappa_0}\right)^{-1} = X^b H^{s+4} , \tag{9}$$

where

$$b = 4 + m[n - (s + 4)(\Gamma_1 - 1)] , \tag{10}$$

and the opacity has the form

$$\kappa \propto \rho^n T^{-s} . \tag{11}$$

If $n = 1, s = 3$, then $b \approx 7$.

With these definitions, the radiative one-zone model was derived in S72. It consists of two nonlinear equations: momentum and energy, and is written here for reference:

$$\frac{d^2X}{d\tau^2} = \frac{H}{X^q} - \frac{1}{X^2} , \tag{12}$$

$$\frac{dH}{d\tau} = \zeta X^{m(\Gamma_1 - 1)} \left(1 - \frac{L_r}{L_0}\right) , \tag{13}$$

where we have taken the luminosity at the base of the shell as fixed for the present analysis. The parameter ζ, the ratio of the free-fall time to the thermal time of the shell (= thermal energy/luminosity), is a measure of the nonadiabaticity of the shell and is the primary parameter of the model. In value, ζ is large in the ionization zones of hot stars, small for cool stars, and near unity in the instability strip.

Stability conditions for this case were also derived in S72:

Dynamic stability if

$$\Gamma_1 > 4/m ; \tag{14}$$

Secular stability if

$$4 + mn + (m - 4)(s + 4) > 0 ; \tag{15}$$

Pulsational stability if

$$b < 0 . \tag{16}$$

Note that a thin shell (large m) is much more stable by the first two criteria. The third criterion is simply a statement about the phasing of the radiative luminosity, and, from equation (10), the three effects outlined by Baker (1966, eq. [35])—geometry (first term), opacity (n and s terms), and "gamma" ($\Gamma_1 - 1$ term)—are very clear. In fact, these criteria agree exactly with Baker's analysis for the case $m = 3$, $\alpha = \delta = 1$ (α and δ are Baker's notation for equation of state exponents). Note that the thin shell factor (m) tends to decrease the importance of the geometrical effect.

b) *Convection*

Two very simple convection schemes have been used in detailed models:

1. "Frozen-in" convection: convection is included in the static structure, but does not vary in time. The above one-zone model is unchanged in this case.

2. "Mixing-length" convection: convection is assumed to conform instantaneously to mixing-length formulae. An extra flux term is added into L_r in equation (13) to account for the convective flux. This flux varies as $\approx r^2 \rho T^{1.5} \approx X^{-10}$ and is a strong stabilizing influence (see, however, Unno and Kamijo 1966, who treat this case and find possible driving in a convective ionization zone).

The model used here includes these extremes as limiting cases. We assume that the rms convective velocity, U', obeys a "phase lag" equation of the form:

$$\frac{\partial U'}{d\tau} = \zeta_c (U_{\rm ml} - U') , \tag{17}$$

where $U_{\rm ml}$ is a mixing-length convective velocity and ζ_c is a "convective efficiency" parameter: the ratio of the free-fall time to a convective adjustment time. Small ζ_c gives the frozen-in case, large ζ_c gives the mixing-length result, with the most interesting value $\zeta_c \approx 1$. We assume her the ζ_c increases toward the red, as convection becomes more efficient and the pulsation

period lengthens, but this assumption may be open to question since the time scale for convective adjustment depends on eddy size, local temperature gradient, and so on, all unknown quantities in a pulsating envelope. Full models (Stellingwerf 1982*b*) suggest that the convection does respond more rapidly toward the red, in response to a larger forcing function (i.e., the difference in radiative and adiabatic temperature gradients). Equation (17) is the one-zone version of equation (28) of Stellingwerf (1982*a*), in a simplified form.

Mixing-length quantities are derived as in Stellingwerf (1982*a*), using the simplest possible assumptions: define the superadiabatic gradient to be

$$\beta = \left(\frac{\partial T}{\partial r}\right)_s - \frac{\partial T}{\partial r} = \frac{T}{H_p}\,\Delta\nabla\,. \tag{18}$$

Here H_p is the pressure scale height, and $\Delta\nabla = \partial \ln T/\partial \ln P - (\partial \ln T/\partial \ln P)_s$ is the usual dimensionless form of this quantity. In the present analysis $\Delta\nabla$ is taken as constant. We then obtain the temperature perturbation:

$$T'_{\rm ml} = 2l\beta = \frac{2l}{H_p}\,T\Delta\nabla \propto T\,, \tag{19}$$

and the mixing-length convective velocity:

$$U_{\rm ml} = \left(\frac{1}{4}\,PQ\,\frac{l}{H_p}\,T'_{\rm ml}\right)^{1/2} \propto T^{1/2}\,, \tag{20}$$

since we have

$$Q = \left(\frac{\partial V}{\partial T}\right)_p \propto \frac{V}{T}\,\frac{\partial \ln V}{\partial \ln T} \propto \frac{1}{p}\,. \tag{21}$$

Using equation (3), we can write

$$\left(\frac{U_{\rm ml}}{U_{\rm ml0}}\right) = X^{-d}H^{1/2}\,, \tag{22}$$

where

$$d = \frac{m}{2}\,(\Gamma_1 - 1) \approx \frac{1}{2}\,. \tag{23}$$

For the convective luminosity, we have

$$L_c = 4\pi r^2 \rho C_p \langle U'T'\rangle\,. \tag{24}$$

To obtain an instantaneous value, use equation (20):

$$T' \propto (U_{\rm ml})^2\;; \tag{25}$$

hence

$$L_c \propto r^2 \rho U'(U')^2\,, \tag{26}$$

$$\frac{L_c}{L_{c0}} = X^{-c}U_c^3\,, \tag{27}$$

where $U_c = U'/U_{\rm ml0}$, and

$$c = m - 2 \approx 8\,. \tag{28}$$

This represents the most conservative choice for L_c in terms of its dependence on mixing-length results. Another choice would be to use equation (19), rather than equation (20), for T'. This gives $L_c \propto X^{-c}U'T$. A third choice, used in Stellingwerf (1982*a*), is the geometric mean of the others, giving $L_c \propto X^{-c}U^2T^{1/2}$. All are equivalent in the limit of large ζ_c (red stars), but differ in the other cases.

For the turbulent pressure, write

$$P_t = \rho(U')^2\,, \tag{29}$$

$$\frac{P_t}{P_{t0}} = X^{-m}U_c^2\,. \tag{30}$$

This term is not explicitly included in the present analysis, but we intend to estimate its effect on stability. The static structure of the envelope is arbitrary in this model, and we represent the convective/radiative splitting by introducing the parameters

$$\gamma_c = L_{c0}/L_0\,, \tag{31}$$

and

$$\gamma_r = 1 - \gamma_c\,, \tag{32}$$

which are adjustable to suit particular models.

The nonlinear convective versions of equations (12), (13), and (17), are

$$\frac{d^2X}{d\tau^2} = \frac{H}{X^q} - \frac{1}{X^2}\,, \tag{33}$$

$$\frac{dH}{d\tau} = \zeta X^{m(\Gamma_1 - 1)}(1 - \gamma_r X^b H^{s+4} - \gamma_c X^{-c}U_c^3)\,, \tag{34}$$

$$\frac{dU_c}{d\tau} = \zeta_c(X^{-d}H^{1/2} - U_c)\,. \tag{35}$$

Linearized forms of the above equations are obtained by putting

$$\begin{aligned} X &= 1 + xe^{\sigma t}\,,\\ H &= 1 + he^{\sigma t}\,,\\ U_c &= 1 + u_c e^{\sigma t}\,, \end{aligned} \tag{36}$$

where the second terms are assumed small, yielding

$$(q - 2 + \sigma^2)x - h = 0\,, \tag{37}$$

$$(\gamma_r b - \gamma_c c)x + [\sigma/\zeta + \gamma_r(s+4)]h + 3\gamma_c u_c = 0\,, \tag{38}$$

$$(d)x - h/2 + (\sigma/\zeta_c + 1)u_c = 0\,, \tag{39}$$

and putting

$$\frac{L_c}{L_0} = (1 + l_c e^{\sigma t})\,,$$

we have

$$l_c = -cx + 3u_c\,. \tag{40}$$

Equations (37) and (39) can be combined to show

$$u_c = \left[\frac{\sigma^2 + m - 4}{2(\sigma/\zeta_c + 1)}\right]x\,, \tag{41}$$

in any nonadiabatic case (i.e. cases with varying h). This equation specifies the phase relationship between the convective velocity and the radius perturbation. For a pulsational root, $\sigma = i\omega \approx i(q-2)^{1/2}$ (quasi-adiabatic), and we obtain the approximate phase relationships (using eqs. [30] and [40]) shown in Table 1.

The two values for L_c and P_t in the $\zeta_c = 1$ case correspond to $m = 10$ and $m = 3$. Note that for $m > 11$, equation (41) changes sign. These phase lags (which can be verified easily by direct integration of eqs. [33]–[35]) provide a rough idea of the stability effects of the convection; there are two effects:

TABLE 1

PHASE LAG OF $(U_c, L_c, P_t)_{max}$ AFTER X_{min}

Parameter	Small ζ_c (Blue)	$\zeta_c \approx 1$ (Instability Strip)	Big ζ_c (Red)
U_c	90°	70°	0°
L_c	0°	4°–13° (damp)	0° (damp)
P_t	0°	2°–7° (drive)	0°

1. Luminosity phasing: we see from Table 1 that the convective luminosity variation is ~180° out of phase with the radius variation for all ζ_c. This phasing will tend to *quench* the pulsation, primarily in the large ζ_c (red) case where the U_c amplitude is appreciable.

2. Turbulent pressure work: Table 1 shows the turbulent pressure 180° out of phase with the radius for both extreme values of ζ_c, but showing a small phase shift tending to that of U_c for $\zeta_c = 1$. This shift will increase the pressure of the shell during the expansion phase and produce positive *driving* for the pulsation. We see that this effect will be the most effective near $\zeta_c = 1$ (near the instability strip). (For thin shells [$m > 11$], the effect is reversed, and we obtain damping.)

The overall qualitative effect should be a slight enhanced instability due to turbulent pressure driving in the instability strip and strong quenching due to convective luminosity "leakage" toward the red. These predictions are in agreement with the detailed results found by Deupree (1977*a–d*) and Stellingwerf (1982*a–b*).

III. STABILITY ANALYSIS

Equations (37)–(39) may be combined to yield a quartic equation in the eigenvalue σ. If we adopt the notation

$$A + B\sigma + C\sigma^2 + D\sigma^3 + \sigma^4 = 0 , \tag{42}$$

we then find

$$A = \zeta\zeta_c[\mathscr{L} + 2\mathscr{S} + 3\gamma_c(2/2 - d)] . \tag{43}$$

$$B = \zeta_c 2 + \zeta(\mathscr{L} + 2\mathscr{S}) , \tag{44}$$

$$C = \zeta\zeta_c(\mathscr{S} + 1.5\gamma_c) + 2 , \tag{45}$$

$$D = \zeta_c + \zeta\mathscr{S} , \tag{46}$$

where

$$\mathscr{L} = \gamma_r b - \gamma_c c , \tag{47}$$

$$\mathscr{S} = \gamma_r(s + 4) , \tag{48}$$

and

$$2 = q - 2 . \tag{49}$$

The stability conditions (such that all roots have negative real part) are due to Hurwitz (Uspensky 1948). For this system, they are

$$A > 0 , \tag{50}$$

$$B > 0 , \tag{51}$$

$$BC - AD > 0 , \tag{52}$$

and

$$D(BC - AD) - B^2 > 0 . \tag{53}$$

By comparison with the radiative case (eqs. [14]–[16]), we expect to find dynamic, secular (thermal), pulsational, and some sort of convective stability criteria. Setting $\gamma_c = \zeta_c = 0$ in equations (43–(46) gives the radiative case and shows that equation (52) is the generalized dynamic stability condition, equation (51) is the secular condition, equation (53) is the pulsational condition, and equation (50) is a new stability condition associated with the convective equation.

a) Turbulent Stability

Expanding equation (43), we find that all references to Γ_1 cancel, and that equation (50) may be represented as a condition on shell thickness ($\zeta\zeta_c \neq 0$):

$$m > \frac{4\gamma_c + \gamma_r(12 + 4s)}{\gamma_c/2 + \gamma_r(4 + n + s)} . \tag{54}$$

This simply duplicates the Jeans condition (eq. [15]) for $\gamma_c = 0$, but requires $m > 8$ for $\gamma_c = 1$. This condition predicts instability if the shell is *too thick*. This is not surprising when compared to the dynamic stability condition in the radiative case (eq. [14]), which shows a similar dependence on shell thickness. This instability, and other convective instabilities to be derived in following sections, will be discussed in § III*e* below.

b) Secular Stability

Using equations (44) and (51), we find

$$\zeta\{\gamma_c(2 - m) + \gamma_r[4 + mn + (m - 4)(s + 4)]\} + \zeta_c(\Gamma_1 m - 4) > 0 . \tag{55}$$

Putting $\zeta_c = 0$, $\gamma_c = 0$, $\gamma_r = 1$, the Jeans condition (eq. [15]) is recovered. Considering the purely adiabatic case ($\zeta = 0$), we obtain $\Gamma_1 > 4/m$—the dynamic stability condition (eq. [14]). Considering the purely convective case ($\gamma_c = 1$, $\gamma_r = 0$), equation (55) becomes

$$\zeta < \left(\frac{\Gamma_1 m - 4}{m - 2}\right)\zeta_c , \tag{56}$$

which implies instability for blue (large ζ) models, although this is, of course, an unphysical case (see below).

c) Dynamic Stability

Expanding equation (52) produces the generalized dynamic stability condition—too lengthy to list here. It reduces to the condition $\Gamma_1 > 4/m$ in the adiabatic ($\zeta = 0$) case, and is always satisfied in the radiative ($\zeta_c = 0$, $\gamma_c = 0$, $\gamma_r = 1$) case. In the purely convective case ($\gamma_c = 1$, $\gamma_r = 0$) with $n = 1$, $s = 3$, $\Gamma_1 = 1.1$, $m = 10$, we find for stability

$$\zeta < \frac{-112 + 19\zeta_c^2 + [9408\zeta_c^2 + (112 - 19\zeta_c^2)^2]^{1/2}}{48\zeta_c} , \tag{57}$$

which, in fact, gives a condition almost identical to equation (56). In the general case ($\gamma_c, \gamma_r \neq 1$), it appears that both conditions (51) and (52) will always be satisfied for reasonable parameter choices.

d) Pulsational Stability

Again, little purpose would be served by exhibiting the expanded form of equation (53). We consider the standard case $n = 1$, $s = 3$, $m = 10$, $\Gamma_1 = 1.1$. With these parameters, the radiative model is pulsationally unstable (radiative damping arising from layers deeper than the single zone is ignored). The effect of gradually increasing the fraction of the flux that is

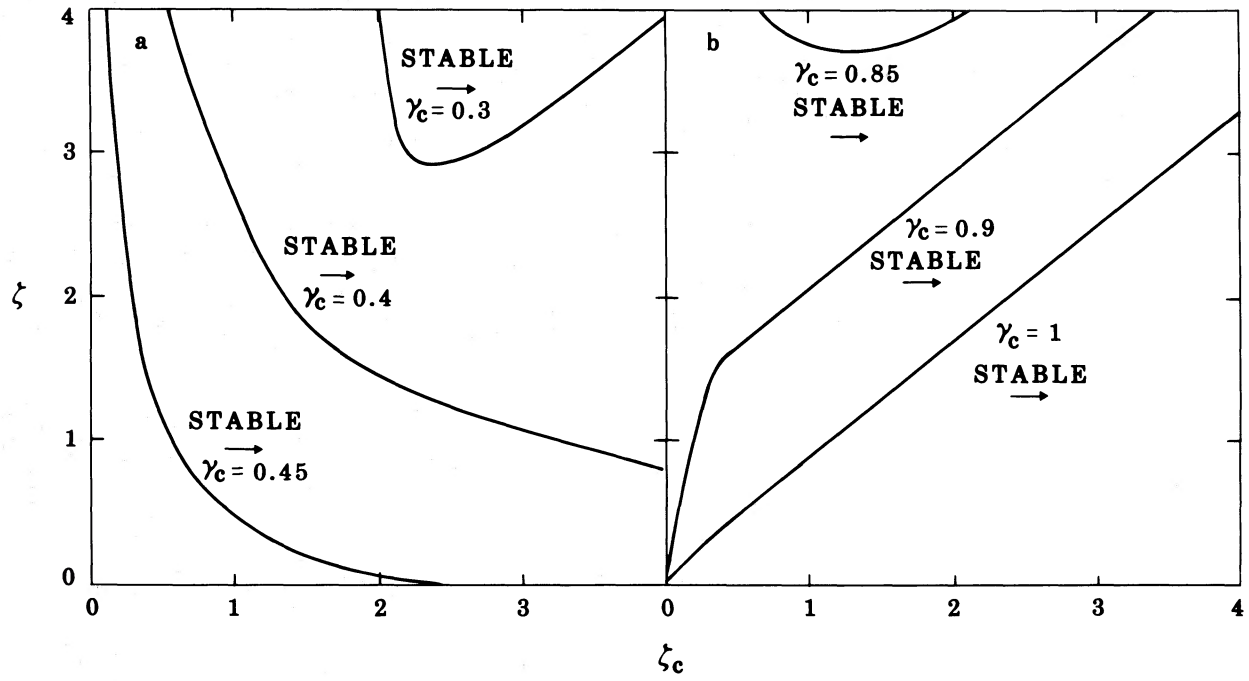

FIG. 1.—Location of stable and unstable regions on the $(\zeta\zeta_c)$-plane for various values of γ_c. See text for details.

carried by convection is shown in Figure 1, on the $(\zeta\zeta_c)$-plane. The locus of reasonable models in this diagram extends from the upper left (blue models) to the lower right (red models), passing through $\zeta = \zeta_c = 1$. We see that the introduction of convection causes a stable region to appear in the upper right of the diagram, and gradually grow in size as γ_c: $0.3 \rightarrow 0.45$. At γ_c all models in the diagram are stable, and this condition persists until $\gamma_c = 0.85$ (shown in Fig. 1*b*). Varying γ_c from 0.85 to 1.0 causes an unstable region to appear at the top of the diagram and to increase in size until, when $\gamma_c = 1$, the condition becomes nearly identical to the secular and dynamic results for this case (eqs. [56] and [57]).

The information in Figure 1 is schematically interpreted in terms of degree of convection in Figure 2. As effective temperature is increased, we expect ζ to increase and ζ_c to decrease. From Figure 1*a*, it appears that all reasonable cases will be stabilized by convection at about $\gamma_c = 0.4$–0.45, as indicated by the shaded region in Figure 2. The convective instabilities found above all occur at high values of ζ and of γ_c and are indicated by the hatched area in the upper left of Figure 2. The dashed line is simply a guess of how much convective flux an actual star will have at any given point in the diagram, based on detailed models. The locus of "real" stars is stabilized by convection toward the red and remains well away from the "dynamic instability" area. The blue edge of the instability strip does not appear, since it is caused by damping in layers deeper than the one-zone shell.

e) Instability in the Completely Convective Case

As we have seen, this model presents a rather curious paradox: although the convection tends to stabilize the pulsation in the majority of cases (see Table 1 and Fig. 2), the completely convective case shows instability in every criterion over a rather wide range of parameters. Equation (54) predicts instability whenever $m < 8$, and the other criteria predict instability when $\zeta \gtrsim (\frac{7}{8})\zeta_c$, for the standard case. The first condition is particularly strong, since it does not depend on the opacity, ζ, ζ_c, or Γ_1 and therefore applies to any star with a sufficiently thick convective shell.

To see how this comes about, consider the linearized equations for the case $\gamma_c = 1, \gamma_r = 0$ (convective flux only):

$$(q - 2 + \sigma^2)x = h \,, \tag{58}$$

$$-cx + (\sigma/\zeta)h + 3u_c = 0 \,, \tag{59}$$

$$(d)x - h/2 + (\sigma/\zeta_c + 1)u_c = 0 \,, \tag{60}$$

from equations (37)–(29). Consider first the case of the "dynamic" instability shown in Figure 2 for large ζ and small ζ_c. Here equation (60) implies $u_c = 0$, so equations (58) and (59) combine to give

$$-c + (\sigma/\zeta)(q - 2\sigma^2) = 0 \,, \tag{61}$$

with the first stability condition:

$$-c = 2 - m > 0 \,. \tag{62}$$

Since m is always greater than 3, this condition is never satisfied. We see that the condition involves the X dependence of the convective luminosity (eq. [40]), and the reason for the instability is the density dependence of the convective luminosity (eq. [24])—the same dependence that is responsible for stabilizing the pulsational root through thermal effects can cause a dynamic runaway situation if convection is present in a nonadiabatic shell. An increase in radius causes a decrease in the convective flux, with an increase in pressure through nonadiabatic heating, and this can drive the instability if ζ is large.

Now consider the effects of time-varying convective flux. Solving for u_c raises the order of the equation to quartic, but the "turbulent" stability condition now becomes

$$-c + (\tfrac{3}{2})(q - 2 - 2d) > 0 \,, \tag{63}$$

or

$$m = d \ln \rho / d \ln r > 8 \,, \tag{64}$$

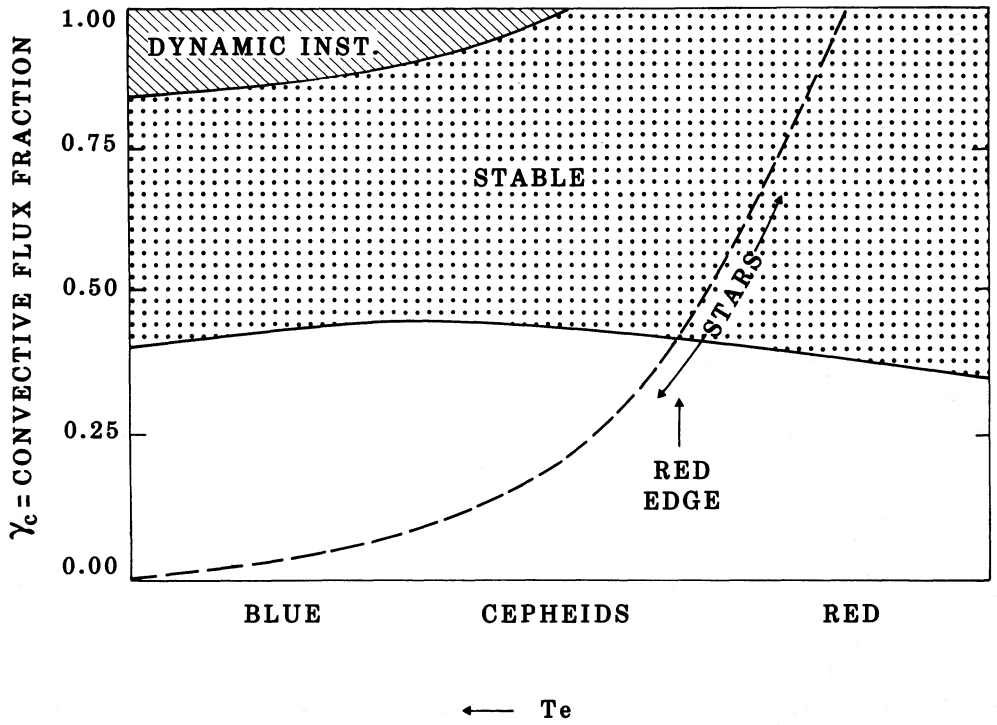

FIG. 2.—Schematic interpretation of Fig. 1 in terms of the effect of varying γ_c for a given star. Actual variable stars lie along the dashed line.

as given by equation (54) for the more general case. Equation (63) contains the same instability mechanism as above as in the first term, with the second term representing the stabilizing influence of the convective flux variation, which can quench the instability if the shell is sufficiently thin (the other stability condition, eq. [62], still appears as the second stability condition). Equation (64) is a general condition for completely convective envelopes: a mixing-length "Jeans condition." For a homogeneous shell, this implies instability whenever the thickness of the shell exceeds 15% of the stellar radius (eq. [4]), but it is more reasonable to consider equation (64) as a local condition on the density variation. If the flux is not completely convective, then equation (54) gives the general condition, and the presence of radiative flux tends to stabilize this effect.

Note that the *radiative* flux also has a strong inverse dependence on the radius perturbation in pulsationally stable regions, but a dynamic instability is avoided because of the strong temperature dependence. Similarly, alternative representations of the convective flux discussed following equation (28) tend to ease, but do not eliminate, this instability, and are probably preferable from a numerical standpoint.

IV. NONLINEAR INTEGRATIONS

The set of nonlinear equations (eqs. [33]–[35]) is easily integrated and provides a check on the above analysis, as well as some insight into the nonlinearities of the system. Three cases were chosen as possible representatives of stars in the vicinity of the Cepheid strip. We emphasize that these choices of parameters are essentially arbitrary, and are not based on detailed models.

Case 1 ("**Blue**"):

$$\zeta = 10\,, \quad \zeta_c = \gamma_c = 0.1\,.$$

Case 2: ("**Strip**"):

$$\zeta = \zeta_c = 1.0\,, \quad \gamma_c = 0.2\,.$$

Case 3: ("**Red**"):

$$\zeta = 0.1\,, \quad \zeta_c = 10\,, \quad \gamma_c = 0.5\,.$$

As indicated in Figure 2, the "**Blue**" and "**Strip**" cases are linearly unstable, and the "**Red**" case is stable. In all cases, we have chosen $n = 1$, $s = 3$, $m = 10$, and $\Gamma_1 = 1.1$. The models were initiated at $X = 1.4$, zero velocity, and integrated using a Runge-Kutta scheme for several periods, or until a reasonably stable oscillation was attained. This rather large amplitude was chosen to intensify nonlinear effects.

The resulting variations of the four variables X, $V = dX/dt$, H, and U_c are shown in Figures 3–5. The three figures cover identical time intervals (scale in units of the free-fall time), so a strong nonlinear effect on the period, which is chiefly a function of amplitude, is evident. The linear adiabatic period for these models is $2\pi/(q-2)^{1/2} = 2.37$; actual periods for the three cases are 3.7, 3.8, and 3.0. The typical Cepheid asymmetry in the radius and velocity variation is also a function of amplitude and is most prominent in Figure 4.

In the "**Blue**" case, Figure 3, the variation of H is large and $\sim 180°$ out of phase with the radius variation, as expected in this case (see eq. [17] of S72), indicating a substantial nonadiabatic contribution to the pressure. Variation of the convective velocity is small and in phase with the shell velocity, in agreement with Table 1. Note that the value of the convective velocity has been "quenched" by the pulsation to ~ 0.85 of its static value. This is a nonlinear effect due to the shape of the radius variation: the mixing-length convective velocity remains low for most of the period, then jumps quite high (a factor of 10) for a brief time near minimum radius. The actual

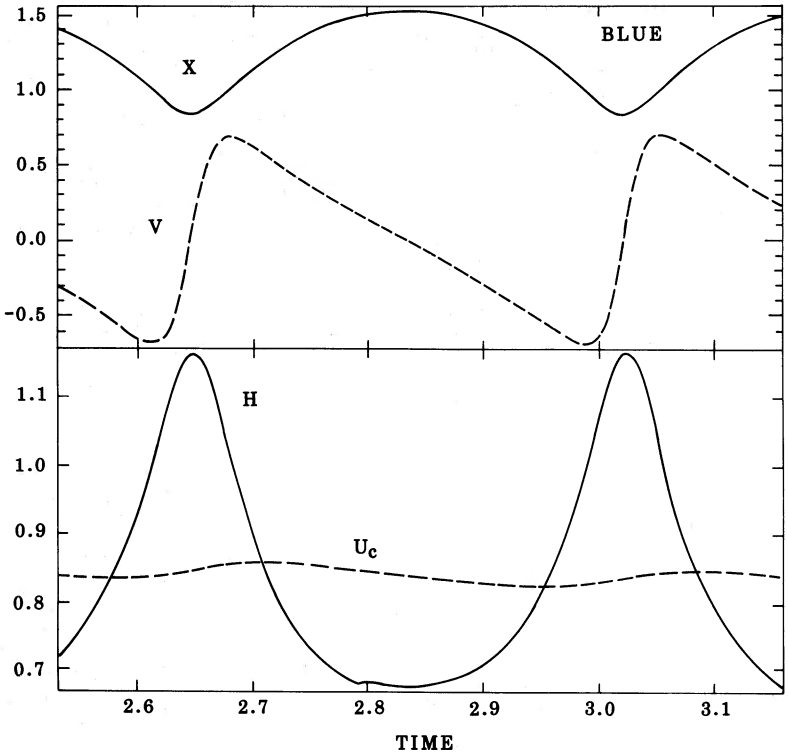

FIG. 3.—Variation of the radius (X), velocity (V), nonadiabatic contribution to the pressure (H), and convective velocity (U_c), for the model designated "Blue" (hot star case).

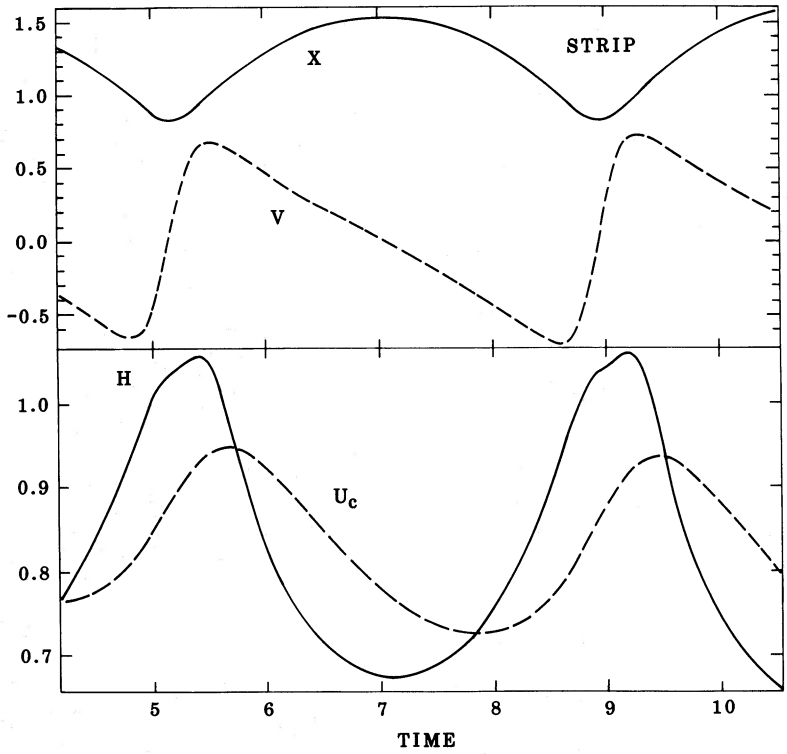

FIG. 4.—Same as Fig. 3, but for the model designated "Strip" (instability strip case)

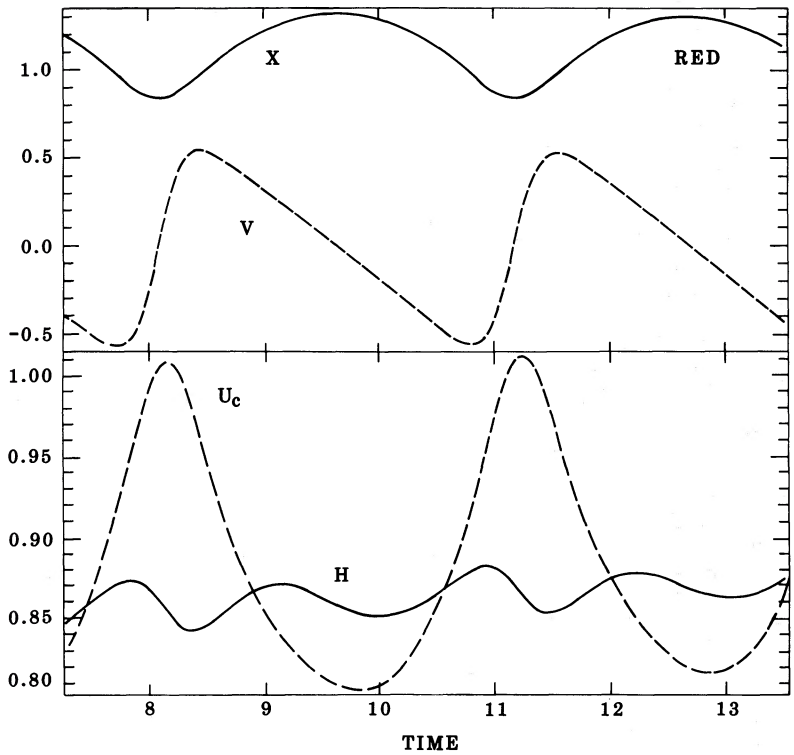

FIG. 5.—Same as Fig. 3, but for the model designated "Red" (cool star case)

convection cannot respond to this short impulse, and so tends to seek a lower value.

In the "**Strip**" model, Figure 4, the phase of H is a bit later and the phase of U_c a bit earlier. The amplitude of H has decreased slightly, while that of U_c has increased significantly. The average value of U_c over the pulsation cycle is ~ 0.85 of the static value. The pulsation has again "quenched" the convection. At a phase just following minimum radius, however, the convective velocity rapidly rises to a value near the static value, after which it again descends. This behavior is seen in the distributed models (Stellingwerf 1984*c*), and in observed stars as well (Benz and Stellingwerf 1985).

In the "**Red**" model, Figure 5, the variation in U_c is very large and 180° out of phase with the radius, again in agreement with Table 1. The variation of H is small in this "adiabatic" case and shows multiple peaks. This is in contrast to the purely radiative case (S72, Eq. [17]) where a 90° phase lag is found.

Figures 6*a*–6*c* shows the H versus X and U_c versus X curves for the three cases, showing the sense (driving or damping) of the contribution of the convective luminosity and turbulent pressure terms to the overall stability of the model. Clockwise motion indicates driving. Figure 6 indicates that the "**Blue**" model is unstable, but only slightly, the "**Strip**" model is very unstable (as clearly seen in the amplitude growth in Fig. 4), and the "**Red**" model shows a stable H variation (also clearly seen in the decaying amplitudes in Fig. 5). These agree with the linear results. All three models show unstable U_c variation, with the largest area loop occurring in Figure 6*b*, as predicted by Table 1.

As an example of the "dynamic" instability for a completely convective shell, Figure 7 shows an integration of a model with $\zeta = 2$, $\zeta_c = 1$, $\gamma_c = 1$, $X_0 = 1.1$, and the other parameters set to standard values. This model lies just within the unstable region in Figure 1*b*, models with lower values of γ_c are expected to be stable, and integrations of these cases show very rapid damping of the pulsation. This unstable model also shows a rapid decay of amplitude at first, but after about two periods the dynamic instability begins to emerge, and a collapse to the origin is the result as seen in Figures 7*a* and 7*b*. The phase plots of H and U_c versus radius are shown in Figures 7*c* and 7*d*. These initially follow a strong damping pattern, then abruptly switch to an exponential runaway solution. Other starting conditions can initiate the runaway in the outward direction, but after several pulsation periods reverse and collapse on the origin. The collapse phase proceeds rapidly to zero pressure in the shell and a halt to the calculation.

As a final example, Figure 8 shows a case of the "thick shell" instability predicted by equation (54). The parameters chosen are $m = 5$, $\zeta = 0.1$, $\zeta_c = 10$, $\gamma_c = 1$, and $X_0 = 1.1$. This is intended to be a fairly reasonable representation of a thick convective shell. The first few periods of the integration showed rapid quenching of the pulsation and little indication of an instability. Figure 8 shows the bahavior at a point at which the original 10% pulsation amplitude had decayed to only a few percent and continues to decay, as seen in the velocity curve. The behavior of the other variables, however, shows the beginning of secular growth characteristic of this instability. In this case the radius continues to increase, reaching values of 4.0 at time 100, and finally ejects the shell.

V. CONCLUSIONS

The model derived here is probably the simplest possible extension of the one-zone model that includes an estimate of time-dependent convection. Mixing-length formulae are used for the convective quantities, and a simple phase lag equation is used for the time dependence. Inspection of the results derived above indicates that the convective effects fall into two

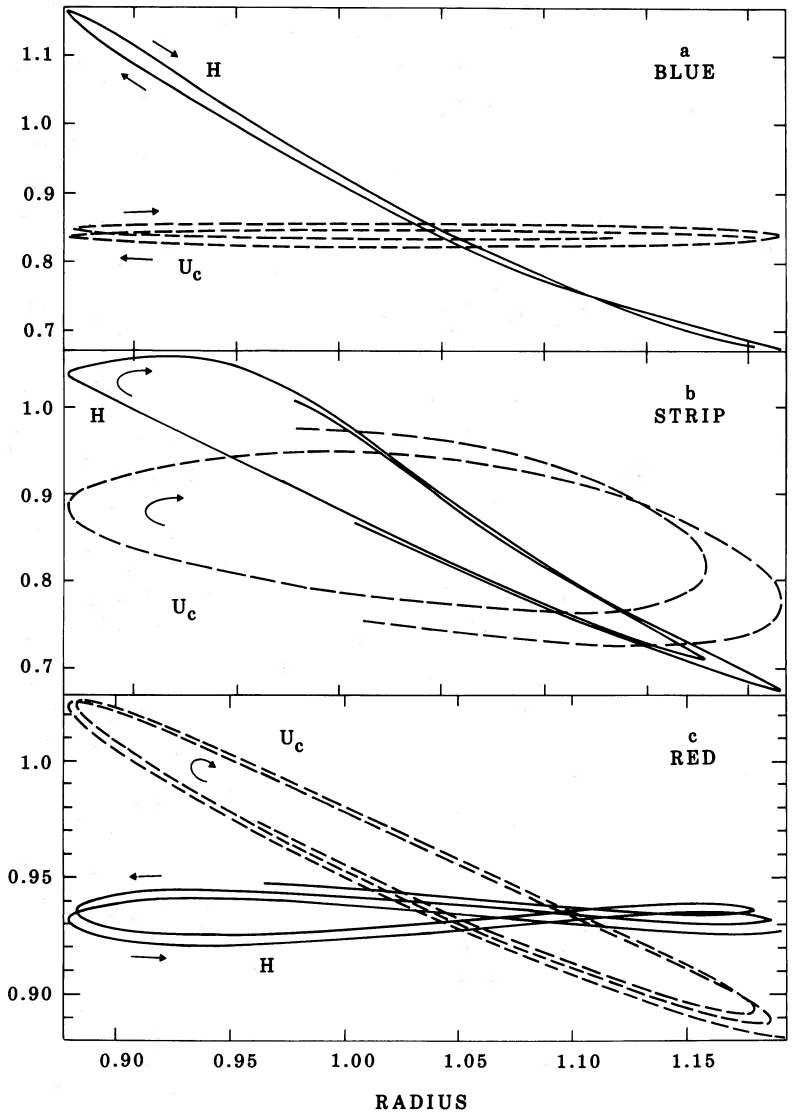

FIG. 6.—Phase plots of the nonadiabatic pressure factor, H, and the convective velocity, U_c, vs. radius for the three cases shown in Figs. 3–5

categories: (1) perturbations to the radiative solution—generally stabilizing the pulsation, but possibly also destabilizing if the turbulent pressure is important; (2) the fully convective case—characterized by strong dynamic instability for thick shells and radiative time scales, pulsational instability at moderate radiative and convective time scales, and strong stabilization at short convective time scales (all relative to the dynamic time). The perturbative effects generally agree with more detailed results and are probably trustworthy. The fully convective case effects must be regarded with some caution, more as indications of the nature of the mixing-length approximation than as physical effects.

The convective effects found in this model include stabilization of the pulsation for red variables, and possible destabilization of bluer variables. Both effects have been seen in the models of Stellingwerf (1984*a*, *b*) and Deupree (1977*c*, *d*). We conclude that these trends are caused by the phasing of the convection in a simple way.

The phase variation of the convection for this model calls for the convection peaking at the phase of minimum radius for red models, and at the phase of maximum velocity for blue models. This is in rough agreement with observations of Cepheids (Benz and Mayor 1982) and with RR Lyrae (Benz and Stellingwerf 1985), although the observations often indicate maximum turbulence just preceding rather than just following the phase of minimum radius. Examination of the detailed model in Stellingwerf (1984*c*) shows that this is caused by the phase shifting in the outer layers such that the ionization zones heat a bit prematurely relative to minimum radius at the surface of the star.

It is hoped that this model can serve as a useful test bed for future implementations of convective theories in pulsating stars. The stability results have been given in some detail for use as a benchmark in these endeavors. Questions that need to be addressed include:

1) How to define the convective time scale;
2) How to modify the mixing-length values to account for thin zones;
3) If it is possible to improve the convective time dependence;
4) What is the best treatment of the convective flux?

Quite likely, these changes and extensions of the theory can be

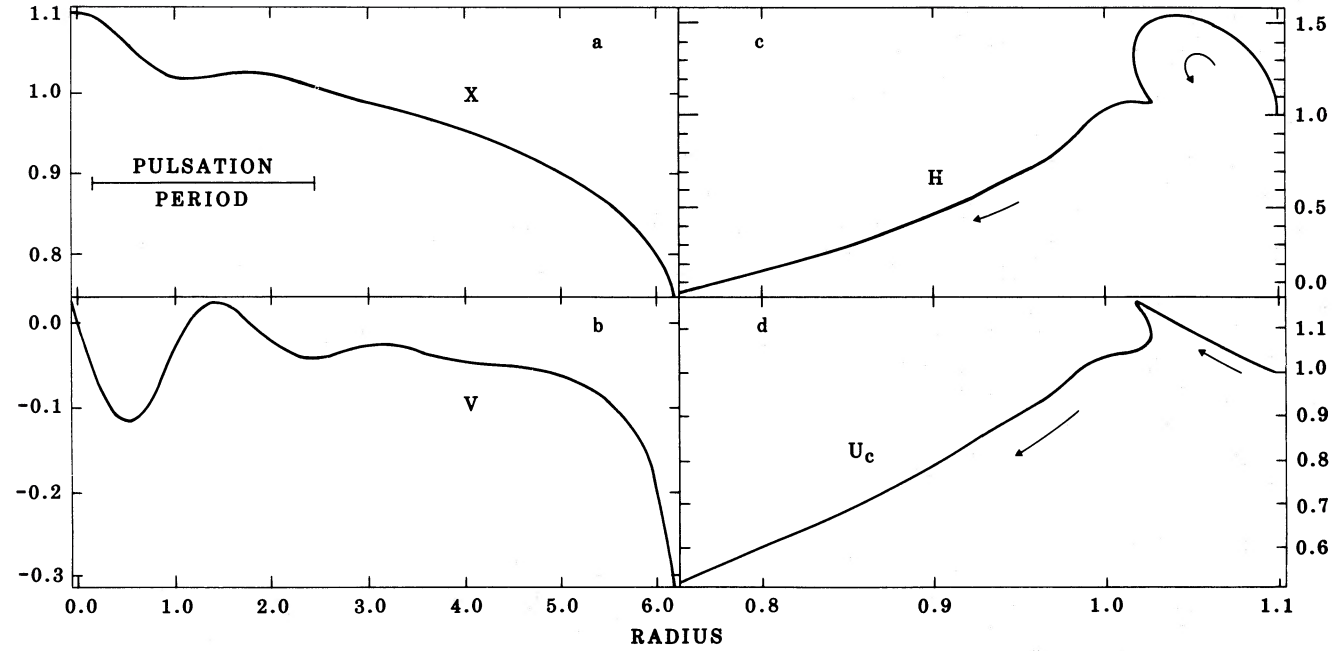

FIG. 7.—Plots of radius (X) and velocity (V) vs. time, and nonadiabatic pressure factor (H) and convective velocity (U_c) vs. radius for the dynamically unstable model discussed in the text.

tested with the one-zone model in a more meaningful way than is possible in a detailed simulation.

In closing, we note that this model contains three independent time scales: pulsation, thermal, and convective. The thermal time scale appears as a growth or decrease in the pulsation amplitude, and the convective time scale could modulate the pulsations in a similar manner, perhaps as observed in the Cepheid HR7308 (Percy and Evans 1980; Burki Mayor, and Benz 1982). Further exploration of the parameter space of the model may reveal such cases.

The author is indebted to Professor N. H. Baker for providing a very thorough review of this manuscript and suggesting many clarifications and simplifications of the model development. This work has been supported by NSF research grant AST84-11029 through Mission Research Corporation.

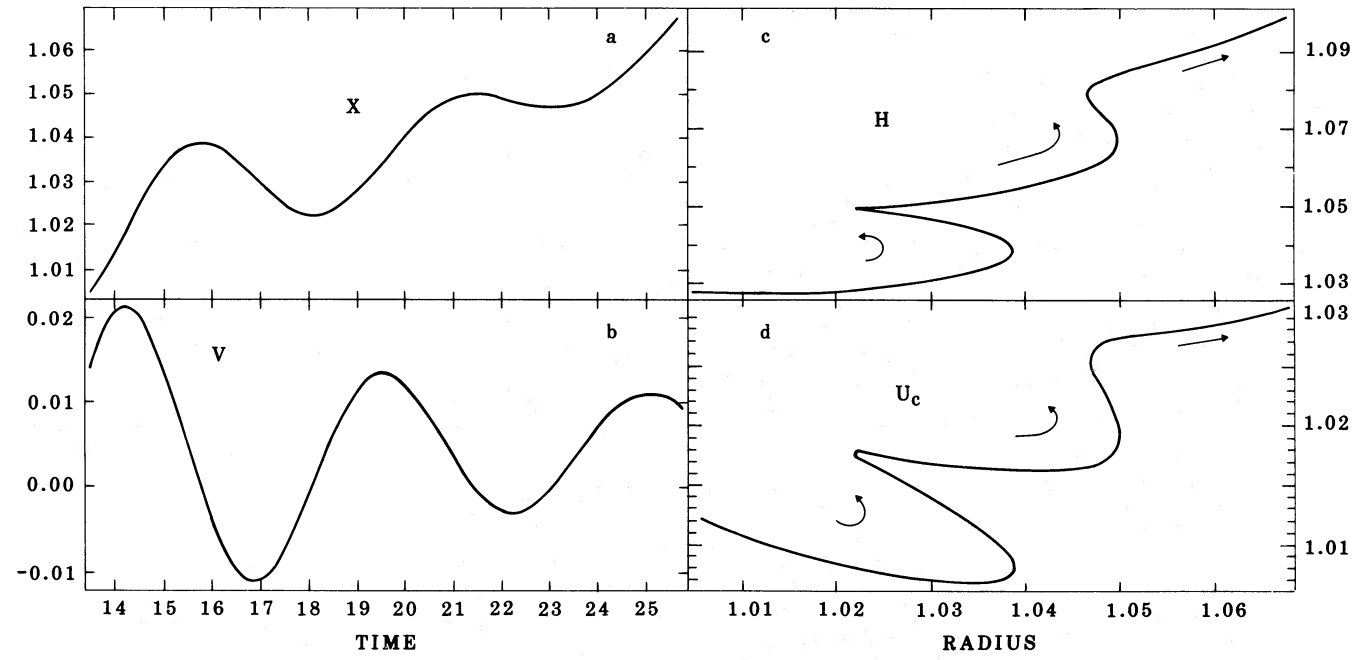

FIG. 8.—Same as Fig. 7, for a model with a thick convective shell

REFERENCES

Auvergne, M., Baglin, A., and Morel, P.-J. 1981, *Astr. Ap.*, **104**, 47.
Baker, N. H. 1966, *Stellar Evolution*, ed. C. Stein (New York: Plenum), p. 333.
Baker, N. H., and Gough, D. O. 1979, *Ap. J.*, **234**, 232.
Baker, N. H., and Kippenhahn, R. 1965, *Ap. J.*, **142**, 868.
Benz, W., and Mayor, M. 1982, *Astr. Ap.*, **111**, 224.
Benz, W., and Stellingwerf, R. F. 1985, *Ap. J.*, **297**, 686.
Böhm-Vitense, E. 1958, *Zs. Ap.*, **46**, 168.
Burki, G., Mayor, M., and Benz, W. 1982, *Astr. Ap.*, **109**, 258.
Cox, A. N., Brownlee, R. R., and Eilers, D. D. 1966, *Ap. J.*, **144**, 1024.
Cox, J. P., Cox, A. N., Olsen, I., King, D. S., and Eilers, D. D. 1966, *Ap. J.*, **144**, 1038.
Deupree, R. G. 1977*a*, *Ap. J.*, **211**, 509.
———. 1977*b*, *Ap. J.*, **214**, 502.
———. 1977*c*, *Ap. J.*, **215**, 232.
———. 1977*d*, *Ap. J.*, **215**, 620.
Gonczi, G. 1981, *Astr. Ap.*, **96**, 138.
———. 1982, *Astr. Ap.*, **110**, 1.
Gough, D. O. 1967, *Ap. J.*, **72**, 799.
King, D. S., Cox, J. P., Eilers, D. D., and Davey, W. R. 1973, *Ap. J.*, **182**, 859.
Percy, J. R., and Evans, N. R. 1980, *A.J.*, **85**, 1509.
Pesnell, W. D. 1985, preprint.
Poyet, J. P., and Speigel, E. A. 1979, *A.J.*, **84**, 1918.
Stellingwerf, R. F. 1972, *Astr. Ap.*, **21**, 91.
———. 1976, *Ap. J.*, **206**, 543.
———. 1982*a*, *Ap. J.*, **262**, 330.
———. 1982*b*, *Ap. J.*, **262**, 339.
———. in *Pulsations in Classical and Cataclysmic Variable Stars*, ed. J. P. Cox and C. J. Hansen (Boulder: JILA), p. 210.
———. 1983, in *IAU Symposium 105, Observational Tests of the Stellar Evolutionary Theory*, ed. A. Maeder and A Renzini (Dordrecht: Reidel), p. 461.
———. 1984*a*, *Ap. J.*, **277**, 322.
———. 1984*b*, *Ap. J.*, **277**, 327.
———. 1984*c*, *Ap. J.*, **284**, 712.
———. 1984*d*, Toronto IAU, ed. B. Madore.
———. 1985, *IAU Colloquium 82, Cepheids: Theory and Observation*, ed. B. F. Madore (Cambridge: Cambridge University Press), p. 280.
Unno, W., and Kamijo, F. 1966, *Pub. A.S.J.*, **18**, 23.
Uspensky, J. V. 1948, *Theory of Equations* (New York: McGraw-Hill).

ROBERT F. STELLINGWERF: Mission Research Corporation, 1720 Randolph Road, SE Albuquerque, NM 87106